Dynamics of microwave-induced currents in ionic crystals

K. I. Rybakov and V. E. Semenov
Institute of Applied Physics, Russian Academy of Sciences, Nizhny Novgorod, 603600, Russia

S. A. Freeman, J. H. Booske, and R. F. Cooper
University of Wisconsin, Madison, Wisconsin 53706

(Received 29 April 1996)

The recent theory of averaged ponderomotive action of microwave fields in solids is expanded to describe quasistationary ionic currents driven by that action. Several limiting cases are explored in detail, and in all cases the effect is shown to depend upon the interfacial properties of the ionic crystal. Experimental results on the dynamics of the microwave-induced currents in AgCl and NaCl are presented. Agreement between experiment and theory provides further and stronger evidence for the general validity of the theoretical model. [S0163-1829(97)02906-8]

I. INTRODUCTION

Over the past decade, results from experimental investigations of microwave processing of materials have repeatedly suggested the existence of an unknown, nonthermal interaction between high-strength microwave fields and ionic materials.[1] Because this nonthermal interaction was originally unanticipated and not fully understood, it has been broadly termed the ''microwave effect.'' For high-temperature ceramic processing experiments involving thermally activated diffusional processes, the common manifestation of the microwave effect is to enhance the process kinetics by either reducing the temperature or the time necessary to complete the process. At first appearance, the experimental results insinuate a possible enhancement of ionic diffusion, although there is no theoretical basis for such a claim.

Freeman, Booske, and Cooper performed ionic conduction experiments[2] that were specifically designed[3] to test for solid-state, bulk (lattice) diffusion enhancements from intense microwave irradiation. The results clearly showed no increase in the bulk diffusion coefficient. Instead, it was found that microwave fields could by themselves induce quasistationary ionic currents to flow in the crystal.

Concurrent to these experiments, Rybakov and Semenov[4] developed a theory that included second-order interactions between high-frequency electrical fields and charged point defects in ionic materials. By application of perturbation methods they showed that oscillatory defect fluxes, driven by the microwave E field, are rectified near crystal surfaces and boundaries. The net result is that charged defects can be driven away from, or pulled towards a surface, producing a near-surface depletion or accumulation. This constitutes a driving force for diffusional flows of defects within the material, which may result in creep deformation[5] and/or formation of quasistationary distribution of electric potential.[6]

This paper describes results of a collaborative effort to verify the validity of the theoretical model by directly applying it to analysis of more recent experimental results. Specifically, an analysis of the temporal nature of the microwave-induced quasistationary (dc) currents is developed and compared with detailed experimental measurements. These dc currents are shown to originate from rectification of the high-frequency currents due to the near-surface second-order interactions similar to those suggested in Ref. 4. The asymmetry between the surface properties at the two ends of the crystal results in a nonzero net current through the crystal.

II. EXPERIMENTAL SYSTEM

A full description of the experimental system appears elsewhere,[3] but a brief description of a slightly modified version is provided here for context. The experimental configuration for measuring microwave radiation effects on ionic currents consists of three subsystems: (1) microwave pulse generation; (2) heating and temperature control; and (3) electronic circuit for measurement of ionic current (no dc bias is applied to the crystal in the results presented here).

The key element of our configuration, where all three subsystems meet, is the waveguide applicator. The inside of the applicator has standard Ku band rectangular waveguide dimensions, and the TE_{10} transmission mode is employed at 14 GHz. The electric field is parallel to the direction of ionic current flow, and the field strength is approximately 10^5 V/m inside the waveguide for 1 kW of microwave power. The microwave power is applied in short, ''single shot'' pulses of approximately 1–10 ms duration.

The waveguide applicator is heated ''conventionally'' using heating tape/strips, a thermocouple, and a temperature controller. The sample is contained within the heated waveguide, and the sample/applicator are not heated (significantly) by the short microwave pulses.

Single crystals of NaCl and AgCl (5 mm $\times$ 5 mm in cross section, 7.5 mm in length) are studied. The ends of the crystals are coated with metallic electrodes. In the case of NaCl, plasma sputtered platinum is used. For AgCl, conductive silver paint is employed. The crystal is then sandwiched in the applicator between two platinum foil electrodes. A gold wire, welded to the Pt foil, conducts the current within the heated region. This current is measured by a Keithley 428 current amplifier which outputs a corresponding voltage to

an oscilloscope. The closed electrical curcuit in which the microwave-induced quasistationary currents flow thus consists of the ionic crystal with the metallic electrodes and the input impedance of the measuring device (current amplifier). The resistance of the ionic crystal is very high compared to the input resistance of the measuring device. The principal delay time in the external circuit derives from op-amps in the current amplifier; these rise times vary in the range 10–100 μs.

The preliminary experiments[2] were specifically designed to test for enhancements of ionic diffusion during microwave irradiation. The approach taken was to first establish an ionic current in the sample (typically NaCl) by applying an external bias across the sample. After several milliseconds, when the current had approximately stabilized to its dc value, the crystal was irradiated by high-strength microwave fields for about 0.5 msec. After this exposure, the ionic current was allowed to stabilize for several more milliseconds before the external bias was turned off.

The important steps taken in the experimental design were to:

(a) heat the crystalline sample by conventional means so that no temperature gradients existed to complicate the analysis;

(b) keep the microwave pulse short so as to not significantly heat the sample by microwave absorption;

(c) apply a constant driving force (essentially the external bias) throughout the experiment, so that the analysis is not complicated by time-varying driving forces such as in diffusion experiments or processing experiments;

(d) maintain a known and controlled electric-field orientation with respect to the sample.

The preliminary results[2] are summarized here. First, an enhancement of the ionic current was observed during the microwave pulse. Second, careful study revealed that this enhancement was unrelated to the applied external bias (driving force). If the microwave fields had acted to increase either the microscopic diffusion coefficient or the defect concentration (i.e., increase the conductivity), then the magnitude of the enhancement would have scaled with the driving forces. This proved that neither the diffusion coefficient nor the defect concentration are significantly affected by microwave fields (for which there was also no theoretical basis). Third, it was determined that the microwave fields seemed to be providing an additional driving force for ionic transport, in effect causing a current that was superimposed upon the ionic current driven by the external bias on the crystal. These observed microwave-induced currents seemed to correspond to the theoretical model.[2]

Finally, it was noted that the experimental system was designed to measure microwave radiation effects on bulk diffusion, and it was not ideally suited for measuring and characterizing this newly discovered phenomenon of microwave-induced currents. There are, however, further investigations possible with the existing system. In the experiments described in this paper, the microwave pulse length is increased by up to 40 times, so that the temporal nature of the induced currents could be studied. The magnitude of the effect is also better characterized versus the electric-field strength. The effect is further observed in AgCl, a material with different defect chemistry.

III. THEORY

The theoretical study of quasistationary electric currents induced in an ionic crystal by a high-frequency (HF) electric field is based on the mathematical model described below. As opposed to Refs. 4 and 5, this model describes the charge (not mass) transport phenomena and includes nonstationary slowly varying processes. The model accounts for diffusion of mobile charge carriers in the solid and their drift in the electric field. The flux of charge carriers is expressed as

$$\mathbf{J} = -D\nabla N + \frac{qND}{kT}\mathbf{E}, \tag{1}$$

where N is the concentration, D is the diffusivity, q is the electric charge of carriers, and $\mathbf{E}$ is the electric-field vector. The Nernst-Einstein relation was used to express mobility in Eq. (1).

As long as action of sources and sinks of charge carriers can be neglected, N and $\mathbf{J}$ are linked by the continuity equation,

$$\frac{\partial N}{\partial t} + (\nabla \cdot \mathbf{J}) = 0. \tag{2}$$

The electric field in the solid is assumed to be quasistatic:

$$\nabla \times \mathbf{E} = 0, \quad (\nabla \cdot \epsilon' \mathbf{E}) = \rho/\epsilon_0, \tag{3}$$

where ϵ_0 is dielectric permittivity of free space, ϵ' is relative dielectric constant of the solid, and the density of free electric charge ρ is determined by the deviations of charge-carrier concentrations N from their equilibrium value in the solid N^0. We assume that in equilibrium $\rho = 0$, and we do not account for the influence of mobile charge carriers on ϵ'.

In a uniform unbounded solid the HF field can cause only HF drift of mobile charge carriers. To obtain a nonzero net (time-averaged) motion of carriers, it is necessary to have ''rectified'' HF currents. Such rectification can take place only due to nonlinear effects associated with nonuniformities in properties of the solid with respect to carrier motion. Interfaces represent a typical example of such nonuniformities. In this study, we consider the nonuniformity associated with the interface of an ionic crystal with metallic electrodes. In accordance with the experimental configuration, we consider the closed nonuniform electric circuit that consists of the ionic crystal, the metallic electrodes, and the measuring device. Most attention will be given to dc current generation processes which take place in the regions of the contact between the crystal and the electrodes.

The analysis of Eqs. (1)–(3) is carried out in one dimension with all vectors directed along the x axis. We assume that there is only one sort of mobile charge carrier in each solid. In particular, in the ionic crystal these are vacancies or interstitials characterized by N_i^0, D_i, and q_i, whereas in the metal these are electrons characterized by N_m^0, D_m, and q_m. We will also consider the contact region between the bulk of the ionic crystal and the electrode as a separate part of the circuit, with the parameters N_c^0, D_c, and q_c. This contact region has the same crystalline structure as the bulk of the ionic crystal; however, it may have different conductivity due to a relatively high concentration of ionic and elec-

tronic defects (introduced when forming electrodes) which can act as electron donors or acceptors. Diffusivities and equilibrium concentrations are assumed to be constant within each of the described parts of the circuit, with the following relationships between them: $D_m \gg D_c$, D_i; $N_m^0 \gg N_c^0$, N_i^0.

The boundary conditions at the interfaces include continuity of the conduction current density $j \equiv qJ$ and the displacement current density $\epsilon_0 \epsilon' \partial E/\partial t$. Also, permeability of the metal-ionic crystal interface S for carrier fluxes is taken into account by introducing kinetic coefficients β_c, β_m:[7]

$$j|_S = q_c \beta_c [N_c|_S - N_c^0] - q_m \beta_m [N_m|_S - N_m^0]. \tag{4}$$

The boundary condition (4) arises due to the difference in crystalline structure of the solids, which ''slows'' carrier fluxes. This does not happen at the boundary between the bulk of the ionic crystal and the contact region, in other words, the kinetic coefficients β are infinitesimally high there.

In the absence of the external electric field there are no charge-carrier fluxes, and the carrier concentrations take their equilibrium values N^0. If the field is not too strong, so that the field-induced deviations of the concentrations from the equilibrium values are small, Eqs. (1)–(3) can be solved by the perturbation method developed in (Ref. 4). Concentration, flux, and field can be presented as follows:

$$\begin{aligned} N &= N^0 + N_1 + N_2 + \ldots, \\ J &= J_1 + J_2 + \ldots, \\ E &= E_1 - \partial\varphi/\partial x + \ldots . \end{aligned} \tag{5}$$

Here $N_1 \equiv \mathrm{Re}[\mathcal{N}\exp(i\omega t)]$ is the first-order HF perturbation of concentration under the field action, N_2 is the second-order quasistationary perturbation. Similarly, $E_1 = \mathrm{Re}[\mathcal{E}\exp(i\omega t)]$ is the HF electric field, φ is the second-order quasistationary electric potential.

Equations (1)–(3) in the first order of the perturbation theory can be presented in the following form:

$$i\omega \mathcal{N} = D \frac{\partial^2 \mathcal{N}}{\partial x^2} - \frac{N^0 D q}{kT} \frac{\partial \mathcal{E}}{\partial x}; \tag{6}$$

$$\partial(\epsilon' \mathcal{E})/\partial x = q\mathcal{N}/\epsilon_0. \tag{7}$$

The (second-order) equations for the quasistationary quantities can be obtained from Eqs. (1)–(3) by averaging over a period of the HF field:

$$\partial \rho_2/\partial t + \partial j_2/\partial x = 0, \tag{8}$$

$$j_2 = -D \frac{\partial \rho_2}{\partial x} - \sigma \frac{\partial \varphi}{\partial x} + \sigma f, \tag{9}$$

$$\frac{\partial}{\partial x}\left(\epsilon' \frac{\partial \varphi}{\partial x} \right) = -\frac{\rho_2}{\epsilon_0}, \tag{10}$$

where $\rho_2 = qN_2$ is the density of quasistationary free charge, $j_2 = qJ_2$ is the density of quasistationary electric current, $\sigma = q^2 D N^0/kT$ is the conductivity associated with mobile charge carriers, and

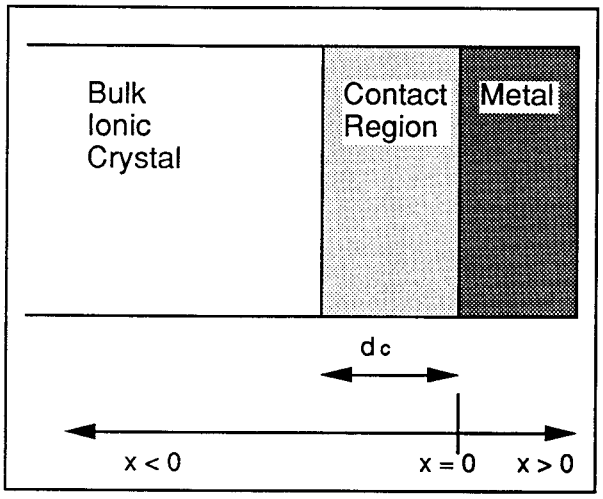

FIG. 1. Graphic representation of the interface region at the end of the crystal and the coordinate axis definition used in the model.

$$f = \frac{\omega}{2\pi N^0} \int_t^{t+2\pi/\omega} N_1 E_1 dt' \tag{11}$$

is the electromotive force (emf) per unit length, caused by the averaged ponderomotive action of the HF field on the carriers. This emf plays the role of a source term in Eqs. (8)–(10). By virtue of Eq. (7)

$$f = \frac{\epsilon_0 \epsilon'}{4qN^0} \frac{\partial |\mathcal{E}|^2}{\partial x} \tag{12}$$

within each part of the circuit.

The sequence of analysis of the described model thus consists of two steps. First, the first-order (HF) Eqs. (6) and (7) should be solved in order to obtain the HF field $\mathcal{E}$ and the ''ponderomotive'' emf f. After that the dynamics of the quasistationary currents can be calculated based on Eqs. (8)–(10).

In the first-order problem, we consider one of the two contacts between the ionic crystal and an electrode. Let the coordinate of the interface between the two crystalline structures be $x = 0$, so that at $x < 0$ there is the contact region within the ionic crystal, and at $x > 0$ there is metal (Fig. 1). Equations (6) and (7) on each side of the interface can be easily transformed into the following equation:

$$\frac{\partial^2 \mathcal{N}}{\partial x^2} = \frac{i\omega\epsilon}{D\epsilon'} \mathcal{N}, \tag{13}$$

where $\epsilon = \epsilon' - i\epsilon''$ is (within our approximation) the complex dielectric permittivity of the solid, and $\epsilon'' = \sigma/\epsilon_0\omega$. The solution of Eq. (13) is

$$\begin{aligned} \mathcal{N} &= n_c \exp(x\sqrt{i\omega\epsilon_c/D_c\epsilon_c'}), \quad x < 0, \\ \mathcal{N} &= n_m \exp(-x\sqrt{i\omega\epsilon_m/D_m\epsilon_m'}), \quad x > 0 \end{aligned} \tag{14}$$

(the square root hereafter is chosen so that its real part is positive). The thicknesses of both the contact region and the metal electrode are much greater than the scale lengths $\sqrt{D\epsilon'/\omega\epsilon}$ on which carrier concentration is perturbed by the

HF field. Therefore, in the HF problem we may consider solely the crystal-electrode contact, not giving attention to other parts of the closed circuit.

The HF electric field, by virtue of Eq. (7), is

$$\mathcal{E}=\mathcal{E}_{c\infty}+\frac{q_c\mathcal{N}}{\epsilon_0}\sqrt{\frac{D_c}{i\omega\epsilon_c\epsilon_c'}},\quad x<0, \tag{15}$$

$$\mathcal{E}=\mathcal{E}_{m\infty}-\frac{q_m\mathcal{N}}{\epsilon_0}\sqrt{\frac{D_m}{i\omega\epsilon_m\epsilon_m'}},\quad x>0.$$

Determining the constants n_c, n_m, $\mathcal{E}_{c\infty}$, and $\mathcal{E}_{m\infty}$ via the boundary conditions listed above, we obtain the following expressions for the HF electric field $\mathcal{E}(x)$:

$$\begin{aligned}
\mathcal{E}&=\frac{E_0}{\epsilon_c}\left[1+\frac{\beta_m(\epsilon_c-\epsilon_m)+(\epsilon_c-\epsilon_c')\sqrt{i\omega D_m\epsilon_m/\epsilon_m'}}{\beta_m\epsilon_m+\beta_i\sqrt{\epsilon_c\epsilon_c'\epsilon_m D_m/\epsilon_m' D_c}+\sqrt{i\omega D_c\epsilon_m/\epsilon_m'}}\exp\left(\sqrt{\frac{i\omega\epsilon_c}{D_c\epsilon_c'}}x\right)\right],\quad x<0,\\
\mathcal{E}&=\frac{E_0}{\epsilon_m}\left[1+\frac{\beta_c(\epsilon_m-\epsilon_c)+(\epsilon_m-\epsilon_m')\sqrt{i\omega D_c\epsilon_c/\epsilon_c'}}{\beta_c\epsilon_c+\beta_m\sqrt{\epsilon_m\epsilon_m'\epsilon_c D_c/\epsilon_c' D_m}+\sqrt{i\omega D_c\epsilon_c/\epsilon_c'}}\exp\left(-\sqrt{\frac{i\omega\epsilon_m}{D_m\epsilon_m'}}x\right)\right],\quad x>0,
\end{aligned} \tag{16}$$

where $E_0=\epsilon_c\mathcal{E}_{c\infty}$ is the amplitude of the external field.

The ponderomotive emf f on the metallic side of the contact is negligible due to high concentration of free electrons [cf. Eq. (12)]. We will only calculate the ponderomotive emf f on the ''ionic'' side of the contact. Assuming that $\epsilon_c''\ll\epsilon_c'$, $\epsilon_m''\gg\epsilon_m'$, $\epsilon_c'\sim\epsilon_m'$, we can rewrite the first equation from Eq. (16) as follows:

$$\mathcal{E}=\frac{E_0}{\epsilon_c'}\left\{1+A\exp\left[\frac{(1+i)x}{l_c}\right]\right\},\quad x<0, \tag{17}$$

where

$$A=\frac{i\beta_m/\omega\lambda_m}{(\beta_c\epsilon_c'/\epsilon_m'\omega l_c)+(1/\epsilon_m')-i[(\beta_m/\omega\lambda_m)+(\beta_c\epsilon_c'/\epsilon_m'\omega l_c)]}, \tag{18}$$

$\lambda_m=\sqrt{D_m\epsilon_0\epsilon_m'/\sigma_m}$ is the Debye-Huckel radius in the metal, and $l_c=\sqrt{2D_c/\omega}$ is the characteristic diffusion length in the contact region of the ionic crystal.

Calculation of f in accordance with Eq. (12) gives

$$f(x)=\frac{\epsilon_0E_0^2}{2\epsilon_c'q_cN_c^0l_c}\left\{|A|^2e^{2x/l_c}+\mathrm{Re}A\cdot e^{x/l_c}\times\left[\cos\left(\frac{x}{l_c}\right)-\sin\left(\frac{x}{l_c}\right)\right]\right\}. \tag{19}$$

Having now solved for the HF field $\mathcal{E}$ and emf f, we can proceed to analyze the quasistationary processes described by Eqs. (8)–(10). For simplicity, we will first ignore the diffusion term in Eq. (9), aiming at only a qualitative description of the dynamics of quasistationary currents. Within this approximation, an analysis of Eqs. (8)–(10) can be carried out in terms of the equivalent circuit shown in Fig. 2. It can be shown that the value of the electromotive force F in this circuit is given by

$$F=\int_{-\infty}^{0}f(x)dx=\frac{\epsilon_0E_0^2}{4\epsilon_c'q_cN_c^0}(|A|^2+2\,\mathrm{Re}A), \tag{20}$$

provided that the conductivity in the contact region where the emf is generated, σ_c, is constant [as follows from Eq. (19), the scale length of this region is l_c]. Not included here is the contribution of the emf generated at the boundary between the contact region with enhanced conductivity and the bulk of the ionic crystal. It can be shown that this contribution is insignificant as long as $\epsilon_i''\ll\epsilon_i'$, $\epsilon_c''\ll\epsilon_c'$, since the total change in the electric field on that boundary is small [cf. Eq. (12)]. According to Eq. (18), the absolute value of the emf F reaches its maximum when $\beta_m/\omega\lambda_m\gg1$, which yields $A\approx-1$. For simplicity, the results in this section imply that this condition is fulfilled. Other parameters of the equivalent circuit are defined in the usual way:

$$R_i=d_i/\sigma_iS,\quad C_i=\epsilon_0\epsilon_i'S/d_i,$$

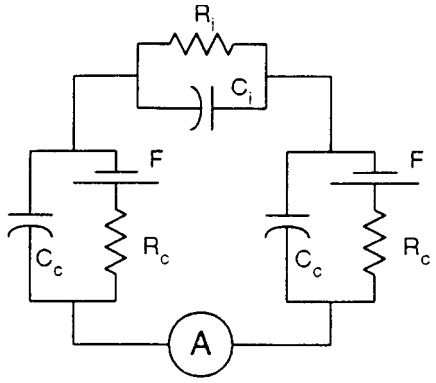

FIG. 2. Equivalent circuit used to model the bulk ionic crystal (subscript i) and the contact region (subscript c) at the ends of the crystals. F is the electromotive force resulting from the ponderomotive action, and A is the current measurement instrumentation.

$$R_c = d_c/\sigma_c S, \quad C_c = \epsilon_0 \epsilon_c' S/d_c, \tag{21}$$

where d_c, d_i are the lengths of the contact region and of the ionic crystal, respectively ($d_c \ll d_i$), and S is the crosssectional area of the crystal. The contribution of the electromotive forces generated at the two contacts in the linear (on the time scale of our quasistationary processes) circuit is additive due to the superposition principle, therefore we will consider only one of them. Being interested in the processes with time scales greater than the time constant of the measuring device, we will assume that the latter does not influence results of the experiment. Under these assumptions, the measured current is given by

$$I = \frac{F}{R_i + R_c} + \frac{F}{R_i + R_c} \frac{R_i C_i - R_c C_c}{R_c C_c} \exp\left(- \frac{R_i + R_c}{R_i R_c} \frac{t}{C_c} \right) \tag{22}$$

(here we used the fact that $C_c \gg C_i$).

If the conductivity (and the dielectric constant) in the bulk of the crystal were the same as in the contact region, then, as seen from Eqs. (21) and (22), the measured current should not depend upon the time. However, in the case when $\sigma_c \gg \sigma_i$ (i.e., $R_c C_c \ll R_i C_i$) the measured current has strong dependence upon the time given by

$$I = \frac{F}{R_i} + \frac{F}{R_c} \frac{C_i}{C_c} \exp\left(- \frac{t}{R_c C_c} \right), \tag{23}$$

or

$$I = \frac{\epsilon_0 S E_0^2}{4 \epsilon_c' q_c N_c^0 d_i} \left[\sigma_i + \sigma_c \frac{\epsilon_i'}{\epsilon_c'} \exp\left(- \frac{\sigma_c t}{\epsilon_0 \epsilon_c'} \right) \right]. \tag{24}$$

Thus, the dynamics of the microwave-induced quasistationary currents are strongly dependent upon the properties of the region within the ionic crystal close to the metallic electrode.

Having completed the analysis of *diffusionless* quasistationary problem, we can now consider the case when *diffusion* in Eq. (9) cannot be neglected. In this case, representation of the contact region of the ionic crystal by the components R_c, C_c, and F would be incomplete. Instead, an element with a more complicated current-potential dependence should be included into the equivalent circuit.

To obtain this dependence, let us note that Eqs. (8)–(10) describe the quasistationary current in the entire closed circuit. From Eqs. (8) and (10) it follows that

$$\frac{\partial}{\partial x} \left[\epsilon_0 \epsilon' \frac{\partial}{\partial x} \left(\frac{\partial \varphi}{\partial t} \right) - j \right] = 0, \tag{25}$$

where the coordinate x is counted along the closed circuit (we will not use the subscript ''2'' here and further). Integrating Eq. (25) and then averaging over the length of the entire circuit (the length-averaged quantities here and further will be denoted by angular brackets $\langle\rangle$), we obtain

$$\epsilon_0 \epsilon' \frac{\partial}{\partial x} \left(\frac{\partial \varphi}{\partial t} \right) - j = - \langle j \rangle (t). \tag{26}$$

Here we used the fact that $\langle \partial \varphi / \partial x \rangle = 0$ since the circuit is closed.

Taking the time derivative of Eq. (9) and using Eq. (26), we obtain the following integrodifferential equation for j within the contact region:

$$\frac{\partial j}{\partial t} = \sigma_c \left[\frac{\partial f}{\partial t} + \frac{\partial}{\partial x} \left(\frac{D_c}{\sigma_c} \frac{\partial j}{\partial x} \right) + \frac{\langle j \rangle - j}{\epsilon_0 \epsilon_c'} \right]. \tag{27}$$

The source term in Eq. (27) is that containing $\partial f / \partial t$. If the HF electric field and therefore the emf f are turned on abruptly, then at the first instance of time after that

$$j(t = 0+, x) = \sigma_c f(x), \tag{28}$$

which can be used as an initial condition for the equation

$$\frac{\partial j}{\partial t} = \sigma_c \left[\frac{\partial}{\partial x} \left(\frac{D_c}{\sigma_c} \frac{\partial j}{\partial x} \right) + \frac{\langle j \rangle - j}{\epsilon_0 \epsilon_c'} \right] \tag{29}$$

that no longer contains a source term.

We will consider Eq. (29) at times which are smaller than the steady-state current establishment time, which is of order of the relaxation time constant in Eq. (22). Obviously, the steady-state current is uniform along the circuit and therefore equal to $\langle j \rangle$. Since the initial current (28) is confined to the contact region (in which the emf f is induced), and since the length of this region is small compared to the length of the ionic crystal, during the steady-state establishment j is much greater than $\langle j \rangle$. Therefore, we will omit $\langle j \rangle$ in Eq. (29). Also, for time scales smaller than $\epsilon_0 \epsilon_c' / \sigma_c$ we can neglect the term j which is responsible for relaxation rather than diffusion of current. As a result, we obtain a diffusion-type equation for the current density j within the contact region:

$$\frac{\partial j}{\partial t} = D_c \frac{\partial^2 j}{\partial x^2}. \tag{30}$$

Since the current on the metallic side of the contact relaxes and becomes equal to the small value $\langle j \rangle$ very rapidly due to the high conductivity of metal, we consider Eq. (30) on the ''ionic'' side (at $x < 0$) with the boundary condition $j(x = 0) = 0$. The initial condition for Eq. (30) is Eq. (28). The solution of Eq. (30) that satisfies these conditions is

$$j = \frac{\sigma_c}{2\sqrt{\pi D_c t}} \int_{-\infty}^{0} f(\xi) \left\{ \exp\left[- \frac{(x - \xi)^2}{4 D_c t} \right] - \exp\left[- \frac{(x + \xi)^2}{4 D_c t} \right] \right\} d\xi. \tag{31}$$

The observed current I on time scales exceeding the delay time of the measuring device is equal to

$$I = S \langle j \rangle \tag{32}$$

[cf. Eq. (27)]. On the other hand, the observed current is also equal to the sum of currents in R_i and C_i:

$$I = C_i \frac{dU}{dt} + \frac{U}{R_i}, \tag{33}$$

where U is the difference of potentials applied to $R_i C_i$. The derivative dU/dt can be obtained by integrating Eq. (26)

over the contact region (we are again considering one of the two contacts) given the current density j within it:

$$\frac{dU}{dt}=\frac{S}{C_c}\langle j\rangle_c-\frac{I}{C_c}, \tag{34}$$

where $\langle j\rangle_c=\int_{-\infty}^{0}j\,dx/d_c$ is the current averaged over the contact region (and in this sense the lower limit of the integration should be understood). Using Eq. (31), we obtain

$$\langle j\rangle_c=-\frac{\sigma_c}{d_c}\int_{-\infty}^{0}f(x)\,\mathrm{erf}\left(\frac{x}{2\sqrt{D_c t}}\right)dx, \tag{35}$$

where $\mathrm{erf}(z)=(2/\sqrt{\pi})\int_0^z\exp(-\eta^2)d\eta$. Since $f(x)$ is localized within the small length l_c from the boundary [cf. Eq. (19)], we may cut the interval of integration at $|x|\ll\sqrt{2Dt}$ and replace $\mathrm{erf}(z)$ with $(2/\sqrt{\pi})z$. Using f from Eq. (19) and performing the integration, we obtain the time dependence of $\langle j\rangle_c$:

$$\langle j\rangle_c=\frac{\epsilon_0 E_0^2\sigma_c}{4\epsilon_c' q_c N_c^0 d_c}\,\frac{1}{\sqrt{2\pi\omega t}}. \tag{36}$$

It should be noted that an expanded form of Eq. (32)

$$I=\frac{d_i}{d_i+d_c}\,\frac{U}{R_i}+\frac{d_c}{d_c+d_i}S\langle j\rangle_c, \tag{37}$$

can also be derived from Eqs. (33) and (34). The closed system consisting of Eqs. (33), (36), and (37), allows us to obtain the time dependence of the observed current I. Its form is generally governed by the parameters σ_i/σ_c (or R_cC_c/R_iC_i, which is the same) and d_c/d_i and can be rather complicated. We will only analyze here some limiting cases.

In the case $\sigma_i/\sigma_c\ll 1$, for $t\ll\epsilon_0\epsilon_c'/\sigma_c$ we obtain

$$I=\frac{d_c}{d_i}S\langle j\rangle_c, \tag{38}$$

or, using Eq. (36),

$$I=\frac{\epsilon_0 S E_0^2\sigma_c}{4\epsilon_c' q_c N_c^0 d_i}\,\frac{1}{\sqrt{2\pi\omega t}}. \tag{39}$$

At $t\sim\epsilon_0\epsilon_c'/\sigma_c$ this dependence passes over into the exponential relaxation with the time constant about $\epsilon_0\epsilon_c'/\sigma_c$ [cf. Eq. (22)].

In the case $d_c/d_i\ll\sigma_c/\sigma_i\ll 1$, Eq. (39) is valid only for $t\ll\epsilon_0\epsilon_i'/\sigma_i$, after which the current increases as $\sqrt{t}$ until it reaches the steady-state value at $t\sim\epsilon_0\epsilon_c'/\sigma_c$.

Finally, in the case $\sigma_c/\sigma_i\ll d_c/d_i$ the observed current displays the same time dependence as in the previous case until $t\sim(\epsilon_0\epsilon_i'/\sigma_i)(d_i/d_c)$, but instead of stabilizing at a steady-state value, it consequently experiences another decrease described by the equation

$$I=\frac{\epsilon_0 S E_0^2\sigma_c}{4\epsilon_c' q_c N_c^0 d_c}\,\frac{1}{\sqrt{2\pi\omega t}}, \tag{40}$$

$(\epsilon_0\epsilon_i'/\sigma_i)(d_i/d_c)\ll t\ll\epsilon_0\epsilon_c'/\sigma_c$. In this case the current reaches its steady-state value at $t\sim\epsilon_0\epsilon_c'/\sigma_c$.

IV. RESULTS AND DISCUSSION

The most important theoretical results can be summarized as follows.

When a contact of an ionic crystal with metal is subjected to the microwave field, a quasistationary (dc) electromotive force (emf) is induced. It is proportional to the microwave power, i.e., to the square of the electric-field strength. This result is consistent with an earlier experimental observation.[2]

The magnitude of the emf is significantly dependent upon the properties of the contact (along with the bulk properties of the ionic crystal and metal). In the typical case of low conductivity of the crystal ($\sigma_c\ll\epsilon_0\epsilon_c'\omega$) and high conductivity of metal ($\sigma_m\gg\epsilon_0\epsilon_m'\omega$) the magnitude of the emf depends mostly upon the kinetic properties of the crystal – metal interface (β_c, β_m) and frequency. As discussed in Ref. 2, the two contacts of the same crystal with the electrodes generally have different kinetic properties, therefore the net emf is nonzero. However, at low frequencies, when $\beta_m/\omega\lambda_m\gg 1$ [cf. Eq. (18)], the contacts become largely equivalent, and the net emf disappears. This may explain why the effect is not observed at frequencies below the microwave range.[2]

The general picture of the temporal dynamics of the quasistationary current correlates with the time profile of the microwave power as follows. When the power is turned on abruptly, the current exhibits a spike with the peak value significantly exceeding the steady state. Then relaxation of the current occurs, until the steady state is established. When the power is turned off, there is a similar spike of the oppositely directed current that is also followed by the relaxation. The second spike is superimposed on the current remaining after the relaxation of the first spike.

The time dependence of the current during relaxation depends upon the properties of the contacts. At times less than $\epsilon_0\epsilon_c'/\sigma_c$ the dynamics of the observed current is determined by diffusional processes within the contact region and may be complicated and not even monotonic, depending on the parameters of the contact region. In fact, this sensitivity of the current dynamics to the physical parameters may be exploited to obtain certain information about the structure of the contact region from data on the current dynamics. On longer time scales, the current may stabilize (if $\sigma_c\ll\sigma_i$) or exhibit further decrease governed by space charge relaxation processes within the contact region. In the simplest case (when the dipolar relaxation processes are not taken into account) the current decreases exponentially, $I\sim\exp(-\sigma_c t/\epsilon_0\epsilon_c')$.

These theoretical predictions are in general agreement with the experimental results. Typical oscilliscope traces of the current (upper trace) and microwave power (lower trace) from the experiments with single crystals of NaCl and AgCl are shown in Figs. 3 and 4, respectively. No bias is applied to the crystal; the current results solely from the application of microwave fields. The oscilloscope is used in the average mode so that the traces in Figs. 3 and 4 are actually an average of 16 separate pulsed experiments. Using the oscilloscope in the average mode effects some smoothing of the traces and enhances the signal-to-noise ratio. Further smoothing is performed before the traces are analyzed.

The results presented here are from a single AgCl crystal

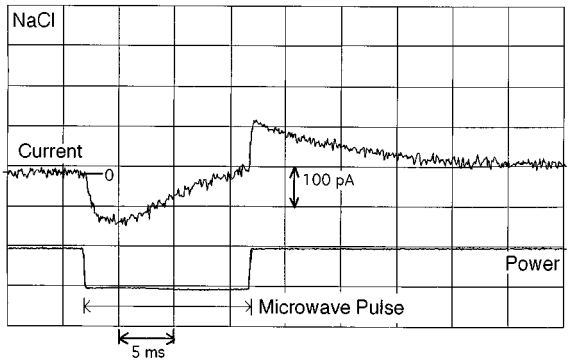

FIG. 3. Oscilloscope traces of the ionic current (upper trace) in a NaCl crystal at 120 °C in response to a pulse of microwave radiation (lower trace). The horizontal scale is 5 ms/div. The vertical scale is 100 pA/div for the current trace.

and a single NaCl crystal. Three AgCl crystals were tested, and approximately ten NaCl crystals were investigated. Each crystal gives qualitatively similar results, but the magnitudes vary within about an order of magnitude. For some crystals, the current signal is virtually impossible to resolve from the noise level. We have hypothesized[2] that the magnitude is dependent on the asymmetric nature of the ends of the crystals.

As is best seen in the results for AgCl (Fig. 4), when the microwave pulse is applied, a large spike of negative current results. This is followed by a relaxation of the current during the pulse. Following the pulse, a spike of positive current occurs and then relaxes back to zero current. As discussed in (Ref. 2), experimentation has shown that the time scales of the relaxations are consistent with ionic diffusion and polarization phenomena. The spikes indicate a very rapid physical response within the crystal and electrodes to the application and removal of the microwave radiation, but the full magnitude of the spikes is likely truncated by the slower rise time of the current amplifier electronics (40 μs for this amplification setting). The initial decay of the spikes (within about 40 μs) shows concave rather than convex curvature, and that is also probably attributable to the amplifier response time. Therefore, it is not until about 100 μs after the spike that the data analysis actually begins. The behavior is slightly different for the initial spike in NaCl (Fig. 3), which appears to respond more slowly to the microwave-induced emf.

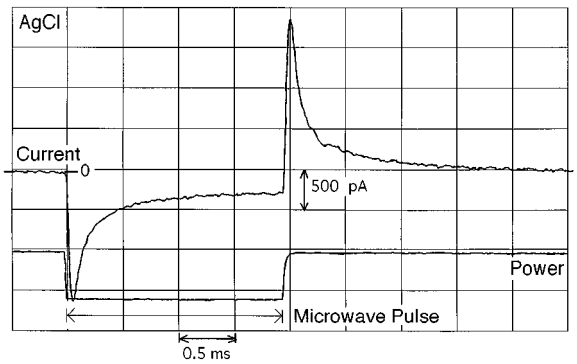

FIG. 4. Oscilloscope traces of the ionic current (upper trace) in an AgCl crystal at 180 °C in response to a pulse of microwave radiation (lower trace). The horizontal scale is 0.5 ms/div. The vertical scale is 500 pA/div for the current trace.

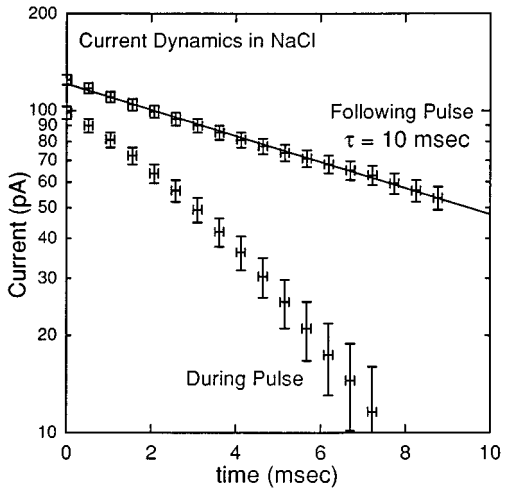

FIG. 5. The current dynamics in NaCl during and following the microwave pulse fit by an exponential decay.

In Fig. 5, the data on the relaxation of the current in NaCl following the microwave pulse (from Fig. 3) are plotted on a logarithmic scale versus time. It can be seen that the relaxation in NaCl following the microwave pulse is exponential to very good accuracy. This is consistent with the theoretical model that does not account for diffusion effects on the current [cf. Eq. (24)]. According to the theory, the time constant of the relaxation should be $\epsilon_0\epsilon_c/\sigma_c$. Calculation of the conductivity in the contact region, σ_c, using the time constant from the experiments ($\sim$10 msec) gives a value 2×10^{-10} (Ohm cm)$^{-1}$. This is about one order of magnitude larger than the bulk conductivity of ''pure'' NaCl at this temperature [which makes Eq. (24) applicable], which suggests that a higher level of impurities exists in the contact region. The difference between the relaxation dynamics during and following the pulse seen in Fig. 5 suggests that the perturbations of carrier concentration in NaCl caused by the microwave field may be not small in the sense of perturbation method applicability.

Evidence for impurities in the contact region is seen in Fig. 6, which shows the Rutherford backscattering spectroscopy (RBS) spectra for the two ends of a NaCl crystal with sputtered platinum electrodes. Analysis of these spectra (and specifically the trailing edge or left side of the Pt peak, which characterizes in part the interface between electrode and halide crystal) using the RUMP/GENPLOT software package indicates that both ends of the crystal have some intermixing of Pt, Na, and Cl over a few hundred Angstroms distance. The difference between the two spectra also offers strong experimental evidence for our claim[2] that the asymmetry of properties at the ends of the crystal leads to our measurement of a net current rather than two equal and opposing currents.

The data from the experiments with AgCl (Fig. 4) are best fit by plotting the current versus $1/\sqrt{t}$, as shown in Fig. 7. For approximately the first millisecond, the time dependence of the current demonstrates excellent agreement with Eq. (40), which results from the theoretical model that covers diffusion effects on the current. After one millisecond, the current dynamics begin to deviate from this model and tend asymp-

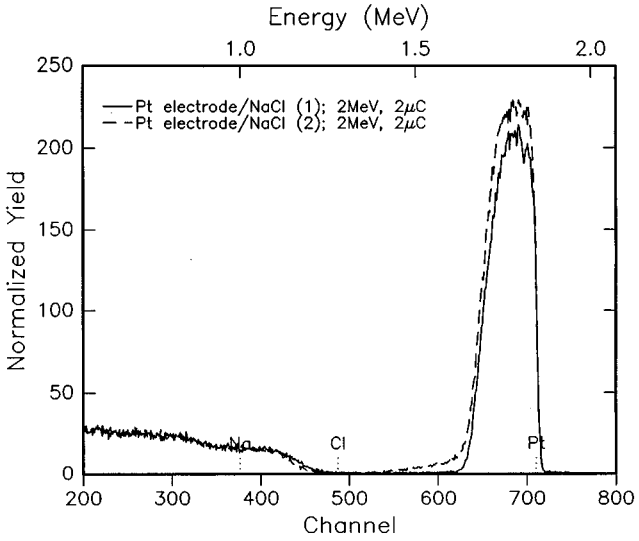

FIG. 6. RBS spectra of the two ends of a NaCl crystal with plasma-sputtered platinum electrodes.

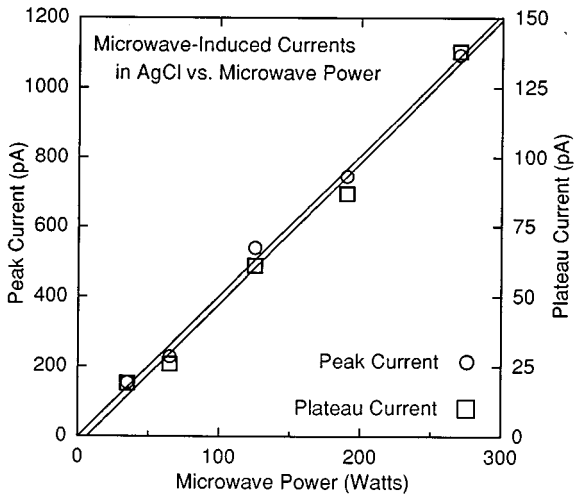

FIG. 8. The magnitude of the current (both peak and plateau) in AgCl depends linearly on power (E_0^2).

totically towards a steady-state current ($\sim$ 200 pA) during the pulse or towards zero current following the pulse, also in agreement with the theoretical expectations. The Ag^+ interstitial defect mobility is sufficiently high in AgCl that one would expect diffusion effects to play out quicker than this, so the fact that this transition is observed at the millisecond time scale suggests that the conductivity in the contact region is much lower than the bulk conductivity of AgCl crystals. A possible reason for such a decrease in the near-surface conductivity may be due to Ag^+ interstitial defects recombining with electrons (from semiconduction-type defects) to form neutral species. In the same vein, the Frenkel defect formation equilibrium could be perturbed near the Ag-painted electrode (due to a lack of free surface), resulting in a lower concentration of Ag^+ defects in the contact region.

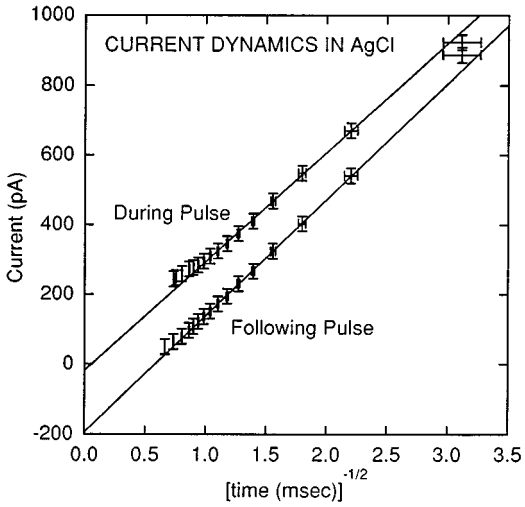

FIG. 7. The current in AgCl during and following the microwave pulse shows a $1/\sqrt{t}$ dependence for the first millisecond before asymptoting towards a steady-state current.

As further evidence for the agreement of the experimental data with the theory, we present in Fig. 8 measurements of the current magnitude versus microwave power. The linear relationship is in agreement with the theoretical model and with earlier results[2] in NaCl. Furthermore, in AgCl the magnitude of the peak current and the magnitude of the plateau current (near the end of the microwave pulse) maintain the same ratio (about 8:1) at all power levels. In other words, the decay dynamics are always the same, regardless of the peak value. This indicates that the crystal-metal contact in AgCl is linear with respect to the quasistationary currents, thus validating the use of perturbation techniques in the theoretical model.

V. CONCLUSIONS

The theory of the averaged ponderomotive action of the HF electric field in solids was applied to description of quasistationary ionic currents induced in ionic crystals by microwave irradiation. Microwave-induced currents in NaCl and AgCl single crystals were studied experimentally. The theoretically obtained dependences of the current upon time and microwave power are in agreement with experimental observations. The theory shows that the magnitude and dynamics of the current greatly depend on the properties of the contact region between the ionic crystal and metal electrode. This has been verified by RBS spectra for NaCl. This is a direct experimental confirmation of the theory that suggests a mechanism of nonthermal influence of HF electromagnetic fields on charge and *mass* transport in solids.

ACKNOWLEDGMENTS

We would like to acknowledge the financial support of the Russian Basic Science Foundation (Grant No. 95-02-05000-a), the National Science Foundation PYI program, the NASA Graduate Student Researcher Program, the Electric Power Research Institute, and the Wisconsin Alumni Research Foundation.

[1] S.J. Rothman, in *Microwave Processing of Materials IV*, edited by M.F. Iskander, R.J. Lauf, and W.H. Sutton, MRS Symposia Proceedings No. 347 (Materials Research Society, Pittsburgh, 1994), pp. 9–18.
[2] S.A. Freeman, J.H. Booske, and R.F. Cooper, Phys. Rev. Lett. **74**, 2042 (1995).
[3] S.A. Freeman, J. Booske, and R. Cooper, Rev. Sci. Instrum. **66**, 3606 (1995).
[4] K.I. Rybakov and V.E. Semenov, Phys. Rev. B **49**, 64 (1994).
[5] K.I. Rybakov and V.E. Semenov, Phys. Rev. B **52**, 3030 (1995).
[6] K.I. Rybakov and V.E. Semenov, in *Solid State Ionics IV*, edited by C.-A. Nazri, J.-M. Tarascon, and M. Schreiber, MRS Symposia Proceedings No. 369 (Materials Research Society, Pittsburgh, 1995), pp. 263–268.
[7] Y.E. Geguzin, *Fizika Spekanija* (Nauka, Moscow, 1984) (in Russian).